Silicon nanowire-array-textured solar cells for photovoltaic application

Chen Chen,[1] Rui Jia,[1,3,a)] Huihui Yue,[1] Haofeng Li,[1] Xinyu Liu,[1] Deqi Wu,[1] Wuchang Ding,[1] Tianchun Ye,[1] Seiya Kasai,[2] Hashizume Tamotsu,[2] Junhao Chu,[3] and Shanli Wang[3]
[1]*Institute of Microelectronics, Chinese Academy of Sciences, Beijing 100029, China*
[2]*Research Center for Integrated Quantum Electronics, Hokkaido University, Sapporo 060-8628, Japan*
[3]*Research Center for Advanced Solar Cells, Chinese Academy of Sciences, China*

(Received 9 June 2010; accepted 24 August 2010; published online 8 November 2010)

In this paper, a vertical-aligned silicon nanowires (Si NWs) array has been synthesized and implemented to the Si NW-array-textured solar cells for photovoltaic application. The optical properties of a Si NWs array on both the plane and pyramid-array-textured substrates were examined in terms of optical reflection property. Less than 2% reflection ratio at 800 nm wavelength was achieved. Using leftover monocrystalline Si (c-Si) wafer (125×125 mm^2), a 16.5% energy conversion efficiency, with 35.4% enhancement compared to the pyramid-array-textured c-Si solar cells, was made by the Si NW-array-textured solar cells due to their enhanced optical absorption characteristics. However, without SiN_x passivation, the short circuit current reduced due to the increased surface recombination when using Si NWs array as surface texturing, indicating that an optimum surface passivation was prerequisite in high-efficiency Si NW-array-textured solar cells.
 [doi:10.1063/1.3493733]

I. INTRODUCTION

Surface texturing is proposed to play an important role in light absorption for solar cells.[1,2] For conventional monocrystalline Si (c-Si) solar cells, it employed micrometer-range pyramid arrays for surface texturing to trap incident solar light. The surface reflection ratio can be reduced to 30% within the whole solar spectra.[3] Recently, nanowire (NWs) arrays structure attracts much attention for solar cell applications due to their enhanced antireflection effects.[4] Also, the radial p-n junction silicon NWs (Si NWs)-based solar cells have been extensively researched in terms of both the physical mechanism[5] and the prototype device fabrication.[6,7] Compared with the planar c-Si structure, vertical-aligned NWs array has reached ultralow reflectance ever reported so far, e.g., less than 3% using a chemical-wet etching technique,[8] ~2.5% developed by reactive-iron-etching method,[9] and less than 2% via vapor-liquid-solid phase growth.[10] In addition, Hu and Chen[11] analyzed the effects of NWs' diameter, length, and wire pitch on the optical absorption property of a Si NWs array by numerical simulation, and revealed that the low optical reflection from NW arrays could be exploited to improve the photon absorption efficiency of solar cells. Up to now, most researches have been merely focused on the optical properties of a NWs array, especially the influence on the reduction in the surface reflectance. However, the c-Si NW-array-textured solar cell is still in its infancy. Moreover, compared with the conventional pyramid-array-textured solar cells, it has not been completed for a detailed study of the effect of a NWs array on other parts of the solar cells, including the surface passivation, electrode contact and the final properties of the cells.

In this paper, a Si NWs array was employed to replace the conventional pyramid-type texturing structure for c-Si solar cells. From the physical mechanism point of view, the effects of the involvement of the Si NWs array on the final properties of solar cells such as the power conversion efficiency (E_{ff}), the open circuit voltage (V_{oc}), the short circuit current (I_{sc}), and the fill factor have been examined and studied.

II. EXPERIMENTAL DETAILS

The leftover p-type (~2.5 Ω cm) c-Si wafer with 125×125 mm^2 cell area was used. All wafers were well-cleaned and removed the surface native oxide layer. Then the surface texturization was performed. There are two kinds of surface texturing structures: the test samples (TSs) with a Si NW array and the control samples (CSs) without the Si NW array. The CSs are used to do the comparison with the TSs. For the TSs, there are four groups (TS-A, TS-B, TS-C, and TS-D), in which the Si NWs array was formed by means of a developed silver-induced wet-chemical-etching process in an aqueous buffered HF and $AgNO_3$ etching solution at 50 °C for about 30 min. The color of the surface with a Si NW array appears black after removing the Ag remnants as possible as we can by immersing the wafers in the concentrated HNO_3 solution. And, the pyramids array was synthesized via the typical anisotropic etching of the silicon in alkaline solution.

In case of the TS-A (five wafers), a NWs array was synthesized prior to the pyramids-array formation to form the hybrid texturing structure. And the SiN_x layer was responsible for the surface passivation. For the TS-B (four wafers), the pyramids array structure was first synthesized prior to the NWs array formation, while other processes were the same as the TS-A. Samples in TS-C (five wafers) were under the same fabrication processes with TS-A, just except the SiN_x deposition. In case of TS-D (four wafers), only a NWs array was formed on the surface of the plane wafers as the

a)Electronic mail: jiarui@ime.ac.cn.

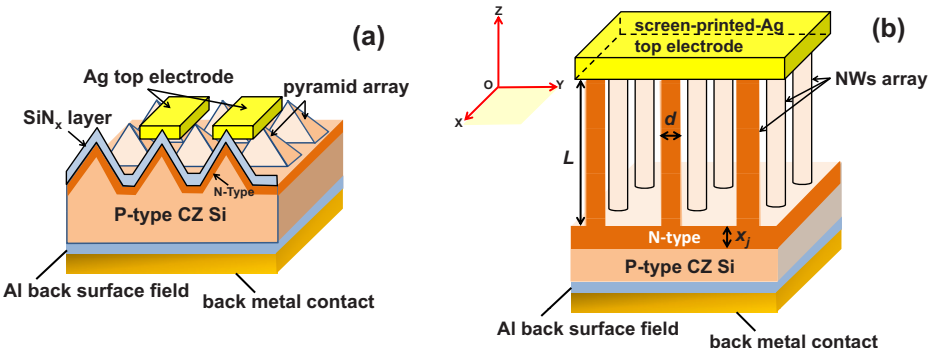

FIG. 1. (Color online) The three-dimensional schematic view of (a) the conventional pyramid-array-textured c-Si solar cells and (b) the Si NW-array-textured solar cells, in which L represents the length of the NWs, d is the diameter of the single NW, and X_j is the junction depth of the p-n junction after phosphorus diffusion.

texturing, with SiN_x layer as the surface passivation. In the CSs, the c-Si solar cells were fabricated following the standard conventional protocols in the CS-C (four wafers) but without texturing process in the CS-A (four wafers), and without SiN_x surface passivation layer in CS-B (four wafers). The aforementioned TSs and CSs were listed in the inset of the Fig. 6(a) together with the fabrication description, accordingly.

Except the surface texturization and the Plasma Enhanced Chemical Vapor Deposition (PECVD)-deposited SiN_x layer, all of the above wafers were under the same fabrication processes, including the n-type phosphorous diffusion to form a p-n junction, Al back-surface-field formation, screen-printed front and back electrode and the electrode metallization.

III. RESULTS AND DISCUSSION

A. The surface morphology of the Si NW-array-textured solar cells

Figures 1(a) and 1(b) show the three-dimensional schematic view of the conventional pyramid-array-textured c-Si solar cells, and the Si NW-array textured solar cells, respectively. In Fig. 1(b), the Si NW-array-textured solar cell consists of a vertical-aligned NW array as surface texturing, where the orange region (the NWs array) is composed of the n-type silicon, and the pink below from the p-type silicon to form the p-n homojunction. As shown in Fig. 2(b), the diameter of an individual NW varies significantly from 50 to 300 nm, with the average diameter of ~150 nm observed from the planar Scanning Electron Microscope (SEM) image. Here, the depth of the p-n junction after phosphorous diffusion was typically ~250 nm in conventional c-Si solar cells. We can thus consider the whole Si NW's region to be primarily n-type after diffusion, and the p-n junction appears underneath the surface of the c-Si substrate.[12] Besides, the hybrid surface texturing structure comprising of both the pyramids array and the Si NWs array was shown in Fig. 2(c). It is worthwhile to note that some of the Si NWs were grown just upon the sidewalls of the pyramids array, which were perpendicular to the (1,1,1) facet of the sidewalls. Moreover, the length of the NWs was proved to be determined by two factors: the etching process duration and the etching temperature. With the increase in either the etching duration or temperature, the Si NWs array becomes longer. In case of our samples etched at 50 °C for 30 min, the height of NWs was set as about 2 μm shown in Fig. 2(a); whereas in conventional c-Si solar cells the height of pyramids was commonly 4–6 μm. The decrease in the features of the Si NW-array-textured solar cells, especially the nanoscaled average diameter of the NWs, substantially lowers the surface reflection ratio and causes the improvement of the final energy conversion efficiency (E_{ff}).

B. Enhanced light absorption property of the Si NW-array-textured solar cells

To examine the optical properties of the wet-chemical-etched Si NWs array, the etching duration-dependent reflection (R) ratio was plotted as a function of incident light wavelength, as shown in Figs. 3(a) and 3(b). At room temperature (300 K), a Si NWs array was separately synthesized on the nontextured and the pyramids-array-textured silicon surface for different etching durations. Then, the R ratios of all samples were measured via ultraviolet spectrophotometer (UV-1700pharmaSpec, by SHIMADZU Inc.®). In Fig. 3(a), compared to the nontextured Si surface, the R ratio of the etched Si NWs array was drastically decreased to less than 5% within the whole interesting wavelength region. As shown in Fig. 3(b), at a wavelength of 800 nm, which is

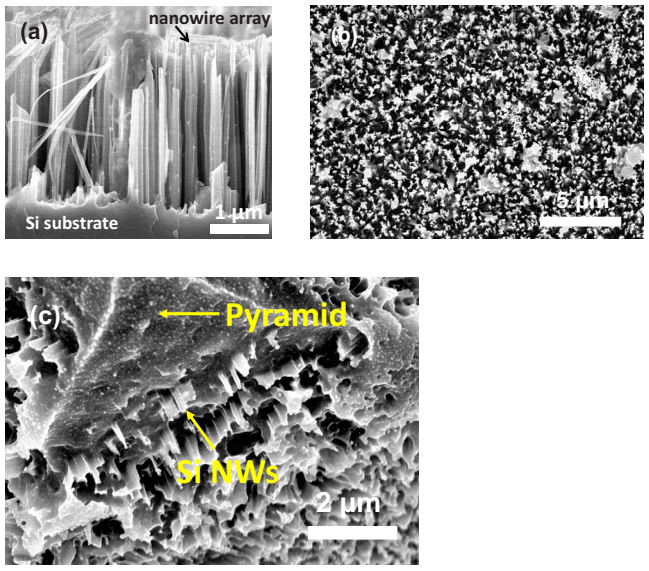

FIG. 2. (Color online) SEM images of (a) the cross-sectional view, (b) plane view, for the etched Si NWs array, and (c) 20° titled SEM image of the hybrid texturing structure comprised of both the NWs array and the pyramids array.

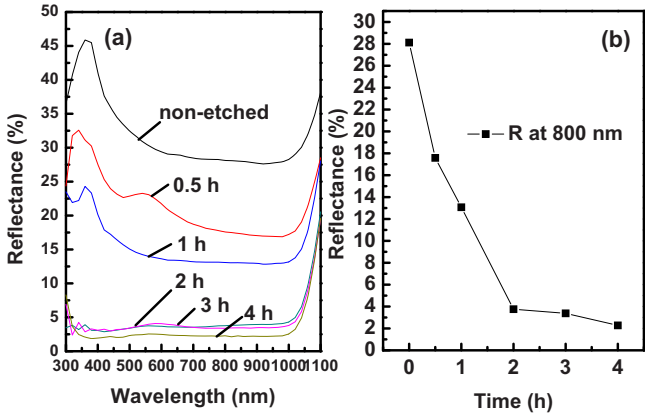

FIG. 3. (Color online) Optical property for the Si NWs array synthesized on the plane silicon surface. (a) The etching duration-dependent reflection (R) ratio as a function of incident light wavelength; and (b) the variation in the reflection ratio (R) with the etching duration.

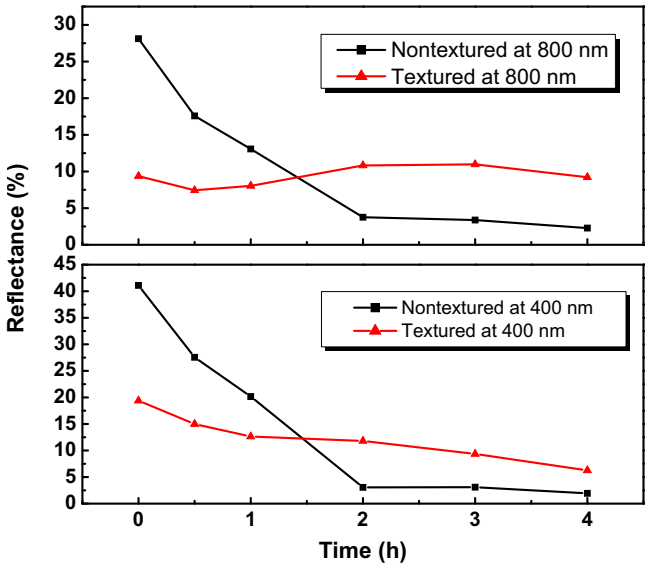

FIG. 4. (Color online) The reflection ratios at the wavelength of 400 and 800 nm for the Si NWs array as the function of the etching duration synthesized on both the plane silicon surface (square symbol) and the pyramid-array-textured surface (triangular symbol).

proven to possess an optimum quantum efficiency for c-Si solar cells,[13] this value can reach around 2%, even if it was synthesized on the plane Si surface. More importantly, when increasing the etching duration from 0.5 to 4 h, the average length of a Si NWs array was increased, making a decrease in the R ratio at the whole wavelengths, especially at 800 nm. However, this trend was alleviated during the last etching time span, e.g., from 2 to 4 h in Fig. 3(b).

This observed reduction in a reflection for the etched samples can be explained from the point of view of wave optics. The incident sunlight will be absorbed by two main mechanisms, the local absorption due to the bulk material, and the light trapping of the surface texturing structure, which eventually takes effect of the reflection ratio. For the plane and surface-polished Si surface, the former mechanism is dominated and the R ratio cannot be restrained. However, in the case of Si NWs array decorated surface, as the diameter of a Si NWs array (~300 nm) becomes comparable to the wavelength of an incident light, e.g., from 300 to 1000 nm, the incident light will be dominantly scattered, which prolongs the optical path length. Therefore, the light trapping is significantly enhanced and the reflection will be evidently suppressed. Such a trend is consistent with the result reported by Hu and Chen,[11] in which the reflection of a Si NWs array is considerably lower than that of the plane silicon thin film. On the other hand, the wire becomes much longer after increasing the etching duration, leading to a reduction in the R ratio. According to the simulation result of the optical absorption for a Si NWs array with different wire length, the absorption edge shifts toward the low energy region, while the absorption for the high energy remains unchanged when increasing the wire length.[11] Therefore, the total optical absorption was believed to be increased. Owing to the reflection is inversely proportional to the absorption, the reflection ratio decreases, as shown in Fig. 3(b). However, effective absorption can only occur within a certain depth below the surface of a Si material, which was denoted as the effective Si absorption depth. The higher photon's energy was, the shallower the absorption would take place, for example, for 1000–1500 nm at 1.5–2 eV down to <100 nm above 3 eV.[14] Therefore, the incident solar photons would not be sufficiently absorbed before being re-emitted from the surface when the wire length exceeded the effective silicon absorption depth whose value is about 1500 nm for Si. Thus, the reflection could not be continuously decreased as the wire length was further increasing.

However, in case of the pyramid-array-textured samples, it is worthwhile to note that the incorporation of a nanoscaled Si NWs array can monotonously reduce the R ratio of the original surface in the short wavelength region, e.g., ~400 nm but first decreases then increases it in long wavelength region, e.g., ~800 nm, as demonstrated in Figs. 4(a) and 4(b). Here, the average diameter of the original pyramids array is commonly 5–10 μm, whereas ~300 nm for a Si NWs array. In short wavelengths, the wavelengths of the incident light are similar to the average diameter of a Si NWs array. Accordingly, the scattering effect would be dominant, and thus significantly suppressed the transmission and decreased the reflection. However, in the long wavelengths, the micrometer scaled pyramids array will facilitate the reflection, whereas the Si NWs array will deteriorate the reflection properties. Therefore, there exists a trade-off for the influence of both the pyramids array and the NWs array on the reflection property for the case of long wavelength region, which results from the first decrease and then the increase in R ratio, as shown in Fig. 4(a). Also, note that after the etching duration exceeds 2 h, the R ratio for the Si NWs textured surface dropped below the pyramids array and NWs array hybrid texturing structure and reached a value less than 2%. It reveals that the reflection reduction using the hybrid texturing structure is not obvious compared to that using the Si NWs array only. We can thus consider the apparent reduction to be primarily due to the involvement of a Si NWs array, which eventually enhanced the absorption of the Si NWs textured c-Si solar cells.

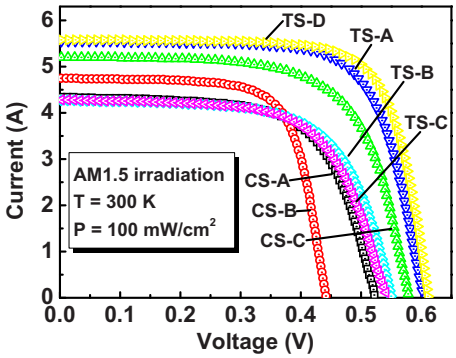

FIG. 5. (Color online) The *I-V* curves of the reference samples (CS-A, B, C) and the TSs (TS-A, B, C, D) under the STC.

C. Photovoltaic property of the Si NW-array-textured solar cells

Figure 5 plots the current-voltage (*I-V*) curves of the reference samples (CS-A, B, C) and the TSs (TS-A, B, C, D) under the standard test condition (STC) (AM1.5 irradiation, $T=300$ K, $P=100$ mW/cm^2). To summarize the I-V characteristics of these samples, the photovoltaic properties of the 125×125 mm^2 NW-textured c-Si solar cells have been demonstrated in Fig. 6 via floating column chart. As shown in Fig. 6, the 35.4% enhancement in E_{ff} for the Si NW-textured c-Si solar cells is achieved in TS-D group with the maximum E_{ff} of 16.5%. The maximum open circuit voltage (V_{oc}) and short circuit current (I_{sc}) appeared in TS-D with 630 mV and 5.58 A, respectively. Compared to the pyramid-textured and SiN_x-passivated c-Si solar cells (CS-C), the involvement of a NWs array in surface texturing can exhibit an incredible enhancement in E_{ff}, for instance: 29.6% for $E_{ff}=15.85\%$, and 35.4% for $E_{ff}=16.55\%$. For the CSs, as both shown in Figs. 5 and 6(a), the elimination of either the pyramid-array-texturing structure or the SiN_x-passivation may dramatically reduce the ultimate energy conversion efficiency of the c-Si solar cells.

In case of the TSs, using the Si NWs array texturing structure (TS-A and TS-D), the short circuit current evidently increased 6.7% compared to that of the c-Si solar cells (CS-C), suggesting the sufficient light trapping characteristics of the Si NWs array. Moreover, with SiN_x passivation, the Si NWs textured (TS-D) solar cells showed higher E_{ff} than the hybrid texturing structure (TS-A, Si NWs array was first synthesized prior to the pyramids texturing) c-Si solar cells, however, this value is shapely reduced in samples of TS-B without SiN_x passivation, demonstrating that the NW geometry provides superior light trapping but also dramatically increases surface recombination, which thus needs excellent surface passivation. In Si NW array-textured solar cells, the carrier recombination losses seem to have strong impact on the ultimate Photovoltaic (PV) properties due to their enlarged surface area of the Si NWs array. Therefore, both the light absorption characteristics and the carrier recombination effect would determine the final PV performance of Si NWs array texturing solar cells. Only increasing the light absorption in Si NWs solar cells does not necessarily means higher energy conversion efficiency. In Fig. 6(c), without SiN_x passivation, the involvement of Si NWs array may reduce the I_{sc} by 2% (TS-C), compared to the samples CS-A using only the pyramids array texturing, revealing that the Si NWs array deteriorate the surface recombination and thus decreasing the I_{sc} of the solar cells. And this is the very reason why the ultimate E_{ff} for the TS-A is a little bit lower than that of the TS-D. On the other hand, the E_{ff} of TS-A with SiN_x-passivation can reach as high as $15.65\pm0.18\%$ with I_{sc} of 5.57 A, however, the E_{ff} exhibits $8.51\pm1.13\%$ with I_{sc} of 4.5 A in TS-C using the same fabrication process except the SiN_x passivation, suggesting that excellent surface passivation is critical in Si NWs array texturing solar cells. Similar trend was also observed by E. Garnett *et al.*,[15] in which the 20-μm-long Si NWs provided only 2% increase in I_{sc} than that of a 8-μm-long Si NWs texturing solar cells. However, this increase is much smaller than the expected 20% increase

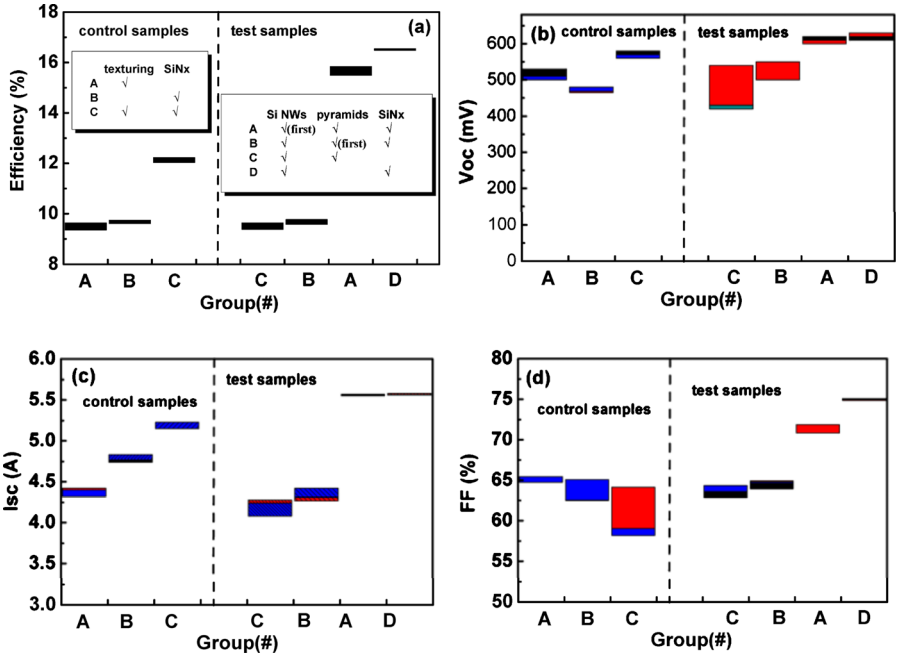

FIG. 6. (Color online) Photovoltaic property of the 125×125 mm^2 NW-textured c-Si solar cells; the inset shows the samples' distribution together with the fabrication description.

in calculation from the pure absorption for such solar cells. Besides, it was also reported that compared to the planar thin film solar cells, the enhancement of the ultimate E_{ff} would be restrained due to their increased surface recombination when prolongating the wire length from 8 to 20 μm. Both of the evidences revealed that other than the optical absorption enhancement, the surface and junction recombination effect also played a critical role in determining the final I_{sc} and the E_{ff} in terms of the Si NW-array-textured solar cells. Additionally, the minority carrier lifetime measurement was carried out to evaluate the surface recombination effect in terms of the Si NWs array based "black silicon" solar cells reported by Srivastava *et al.*[16] It revealed that the surface recombination velocity of minority carriers generated in Si NWs array was much faster than that of bulk crystalline silicon, and the minority carrier lifetimes decreased remarkably (about two to three times) as compared with the original silicon wafers. The ultrahigh surface area of the Si NWs array with high density of surface defects was attributed to the possible reason. Therefore, to further improve the ultimate performance such as E_{ff}, V_{oc}, and I_{sc}, optimum surface passivation recipes would be explored to suppress the increased recombination effect in the Si NW-array-textured solar cells.

IV. CONCLUSION

In this paper, a vertical-aligned Si NWs array was synthesized by means of a simple chemical-etching method on both the plane and pyramid-array-texturing c-Si surface, then it was embedded to form the Si NW-array-textured solar cells. The optical properties of this Si NWs array on both substrates were examined in terms of optical reflection property. Less than 2% reflection ratio at 800 nm wavelength was achieved in Si NWs array samples without other surface texturing. PV characteristics of the Si NW-array-textured solar cells were investigated. As a result, 16.5% E_{ff}, with 35.4% enhancement compared to the pyramid-array-textured c-Si solar cells, was achieved due to their excellent optical absorption characteristics. However, for Si NW-array-textured solar cells, 2% decrease in I_{sc} for samples without SiN_x passivation proves that both optical absorption and the surface recombination play the critical roles in determining the final PV property. Therefore, optimum surface passivation recipes would be necessary for high energy conversion-efficiency Si NW array-textured solar cells.

ACKNOWLEDGMENTS

This work was subsidized by the 973 Projects under Grant Nos. 2006CB604904 and 2009CB939703, by the Chinese NSF under Grant Nos. 60706023, 60676001, 90401002, and 90607022, by CAS under Grant No. YZ0635, and under the Chinese Academy of Solar Energy Action Plan, China. Also this work was also subsidized by PRESTO, Japan Science and Technology Agency, 4-1-8, Honcho, Kawaguchi-shi, Saitama 332-0012, Japan.

[1] M. A. Green, Z. Jianhua, A. Wang, and S. R. Wenham, IEEE Trans. Electron Devices **46**, 1940 (1999).
[2] J. Zhao, A. Wang, and M. A. Green, Prog. Photovoltaics **7**, 471 (1999).
[3] D. L. King and M. E. Buck, *Experimental optimization of an anisotropic etching process for random texturization of silicon solar cells*,Proceedings of 22nd Conference Record of IEEE Photovoltaic Specialists Conference, Las Vegas, NV, 7–11 October, 1991, Vol. 1, p. 303.
[4] L. Tsakalakos, J. Balch, J. Fronheiser, M. -Y. Shih, S. F. LeBoeuf, M. Pietrzykowski, P. J. Codella, B. A. Korevaar, O. V. Sulima, J. Rand, A. Davuluru, and U. Rapol, J. Nanophotonics **1**, 013552 (2007).
[5] B. M. Kayes, H. A. Atwater, and N. S. Lewis, J. Appl. Phys. **97**, 114302 (2005).
[6] L. Tsakalakos, J. Balch, J. Fronheiser, B. A. Korevaar, O. Sulima, and J. Rand, Appl. Phys. Lett. **91**, 233117 (2007).
[7] B. Tian, X. Zheng, T. J. Kempa, Y. Fang, N. Yu, G. Yu, J. Huang, and C. M. Lieber, Nature (London) **449**, 885 (2007).
[8] K. Peng, Y. Xu, Y. Wu, Y. Yan, S.-T. Lee, and J. Zhu, Small **1**, 1062 (2005).
[9] W.-L. Min, B. Jiang, and P. Jiang, Adv. Mater. **20**, 3914 (2008).
[10] J.-Y. Yang, C.-W. Liu, C.-L. Cheng, J.-T. Jeng, B.-T. Dai, J.-S. Lin, and K.-C. Chen, IEEE Electron Device Lett. **30**, 1299 (2009).
[11] L. Hu and G. Chen, Nano Lett. **7**, 3249 (2007).
[12] E. C. Garnett, Y.-C. Tseng, D. R. Khanal, J. Wu, J. Bokor, and P. Yang, Nat. Nanotechnol. **4**, 311 (2009).
[13] S. M. Sze, *Physics of Semiconductor Devices*, 2nd ed. (Wiley, New York, 1981), Chap. 14, p. 812.
[14] R. A. Street, P. Qi, R. Lujan, and W. S. Wong, Appl. Phys. Lett. **93**, 163109 (2008).
[15] E. Garnett and P. Yang, Nano Lett. **10**, 1082 (2010).
[16] S. K. Srivastava, D. Kumar, P. K. Singh, and V. Kumar, *Silicon nanowire arrays based "black silicon" solar cells*, Proceedings of 34th Photovoltaic Specialists Conference (PVSC), Philadelphia, PA, 7–12 June 2009, p. 001851.